Received: 12 October 2020 | Revised: 17 March 2021 | Accepted: 15 April 2021

DOI: 10.1002/psp4.12644

TUTORIAL

Understanding effect site pharmacology of uprifosbuvir, a hepatitis C virus nucleoside inhibitor: Case study of a multidisciplinary modeling approach in drug development

Paul van den Berg[1] | **Wei Gao**[2] | **Maurice J. Ahsman**[1] | **Leticia Arrington**[2] | **Filippos Kesisoglou**[2] | **Randy Miller**[2] | **Teun M. Post**[1] | **Matthew L. Rizk**[2]

[1]LAP&P Consultants BV, Leiden, The Netherlands

[2]Merck & Co., Inc., Kenilworth, New Jersey, USA

Correspondence
Paul van den Berg, LAP&P Consultants BV, Archimedesweg 31, 2333 CM Leiden, The Netherlands
Email: P.vandenBerg@lapp.nl

Funding information
Merck Sharp & Dohme Corp., a subsidiary of Merck & Co., Inc., Kenilworth, NJ, USA, funded the work described. No external funding was obtained for this project.

Abstract

Uprifosbuvir is a uridine nucleoside monophosphate prodrug inhibitor of the hepatitis C virus NS5B RNA polymerase. To quantitatively elucidate key metabolic pathways, assess the link between unmeasurable effect site concentrations and viral load reduction, and evaluate the influence of intrinsic and extrinsic factors on pharmacokinetics and pharmacodynamics, a model-informed drug development (MIDD) framework was initiated at an early stage. Originally scoped as a modeling effort focused on minimal physiologically based pharmacokinetic and covariate analyses, this project turned into a collaborative effort focused on gaining a deeper understanding of the data from drug metabolism, biopharmaceutics, pharmacometrics, and clinical pharmacology perspectives. This article presents an example of the practical execution of a MIDD-based, cooperative multidisciplinary modeling approach, creating a model that grows along with the team's integrated knowledge. Insights gained from this process could be used in forming optimal collaborations between disciplines in drug development for other investigative compounds.

INTRODUCTION

The preclinical and clinical (phase I, IIa, IIb) steps of the drug development process are geared toward obtaining an understanding of safety and efficacy of a new compound, providing confidence in the compound's suitability for prospective patients. Studies are designed to answer specific questions, thereby providing the development team with useful data on various aspects of the drug's mechanism of action, pharmacokinetics (PK), and exposure–response profile.

Despite these efforts, it is not always possible to provide a complete picture based on the results of individual studies alone, particularly for drugs with a complex and partially unexplained metabolism or mechanism of action and drugs for which exposure at the site of action cannot be measured. Population PK and pharmacodynamic (PD) modeling can be used to test different hypotheses on unexplained aspects of drug kinetics and dynamics provided there is enough informative data from preclinical experiments and clinical studies. The traditional pharmacometric approach leverages empirically observed concentrations or effects data collected from preclinical and clinical studies. The data-driven nature tends to lead to descriptive models for the specific compounds. Due to limited data, incorporating information around drug

Paul van den Berg and Wei Gao are co-first authors.

metabolism pathways and/or the drug mechanism of action in the traditional pharmacometric approach could be challenging, especially when there is a lack of data or limited mechanistic understanding. As such, the traditional pharmacometric approach presents challenges such as difficulty of direct extrapolation to other compounds or extension to include new insights in biological mechanisms, which limits the usefulness beyond answering the initial questions on which the model was based and constraining the "learn and confirm" value of the quantitative approach. Systems pharmacology models may overcome some of these shortcomings and facilitate better iteration between experiment and model, but models that fully describe the underlying biology or pharmacology tend to suffer from problems with parameter identifiability, lack of certainty in particular parameter values, and computational limitations as well as limitations on our understanding of causal biology. Combining the best characteristics of the pharmacometric and systems pharmacology approaches together with the relevant development questions can provide the best starting position; the integration of known or presumed mechanistic information from a variety of sources into a pharmacometric model framework could maximize the chance to answer key questions while maintaining the flexibility to incorporate new data or insights. When combined with intensive multidisciplinary feedback and subject matter expertise, this allows construction of a model that "grows" along with the increased understanding of the compound and relevant mechanisms, thereby simultaneously being informed by and informing experts in different disciplines within the development team, essentially serving as a quantitative knowledge repository.

Compound under development: uprifosbuvir

Uprifosbuvir is a uridine nucleoside monophosphate prodrug inhibitor of the hepatitis C virus (HCV) NS5B RNA polymerase, which was under development as a component of an effective direct-acting antiviral combination therapy regimen for chronic HCV infection. Based on preclinical data and the reported clinical PK and PD of other HCV nucleoside inhibitors, the following main metabolic routes and likely mechanism of action were considered during model development: following the metabolism of uprifosbuvir to the monophosphate form in the liver, it is activated by phosphorylation to form the pharmacologically active nucleoside triphosphate (NTP). NTP, in this context, is the collective term for cytidine triphosphate (CTP) and uridine triphosphate (UTP). Presumably, intracellular NTP, CTP, and/or UTP could be linked to efficacy (reduction of viral load [VL]), but because they do not circulate in plasma and direct measurement of liver nucleoside levels is technically not feasible in a clinical trial setting, a direct link could not be established. Metabolites of phosphorylated nucleosides can be assayed in plasma, and some have suspected that these metabolites could be considered as biomarkers for hepatic CTP and UTP activity; the metabolite M5 in plasma could reflect hepatic phosphorylated cytidine varieties (CXP), whereas M6 could be linked to their uridine equivalents (UXP).

A model-informed drug development (MIDD) framework was initiated to quantitatively elucidate key pathways of the complex metabolism of uprifosbuvir to assess the optimal link to VL reduction and to evaluate the influence of different intrinsic and extrinsic factors on PK and PD. Intensive engagement of experimentalists and clinicians was considered desirable not only to inform the model-building process but also to inform the discussions on the metabolism in iterations with preclinical and clinical experts.

This work represents a MIDD case study to illustrate a cooperative modeling approach in which hypothesis testing, input from experimentalists and clinicians, feedback from different stakeholders, and continuous reevaluation of the model have been used to characterize the metabolism and effect site exposure of a drug with complex pharmacokinetics. We place emphasis on the chronology and impact of multidisciplinary cooperation, focusing on a high-level overview of the process without overwhelming the readers with pharmacometric details.

METHODS

Scoping of MIDD framework

We started the model-based approach at a crucial point in the development track, at a time when the following two processes converged:

1. A general schematic of suspected uprifosbuvir metabolic pathways was hypothesized based on existing knowledge of nucleoside kinetics in combination with a number of *in vitro* experiments (Figure 1b). However, there was considerable uncertainty in the translation to the *in vivo* situation, especially considering the large number of potential metabolic routes and the unknown contribution of each individual metabolic pathway to the overall kinetics of uprifosbuvir and its metabolites. Central to the preliminary picture was the assumption that uprifosbuvir would be absorbed from the gut, enter the hepatocytes, and undergo intrahepatocyte metabolism forming M5 and M6 via pharmacologically active CTP and UTP. In detail, this process occurs via cleavage of uprifosbuvir resulting in M4 and subsequently uridine monophosphate (UMP). UMP can be metabolized into M6, but can also be phosphorylated to UTP, thereby entering a cyclical process in which UTP is sequentially converted into

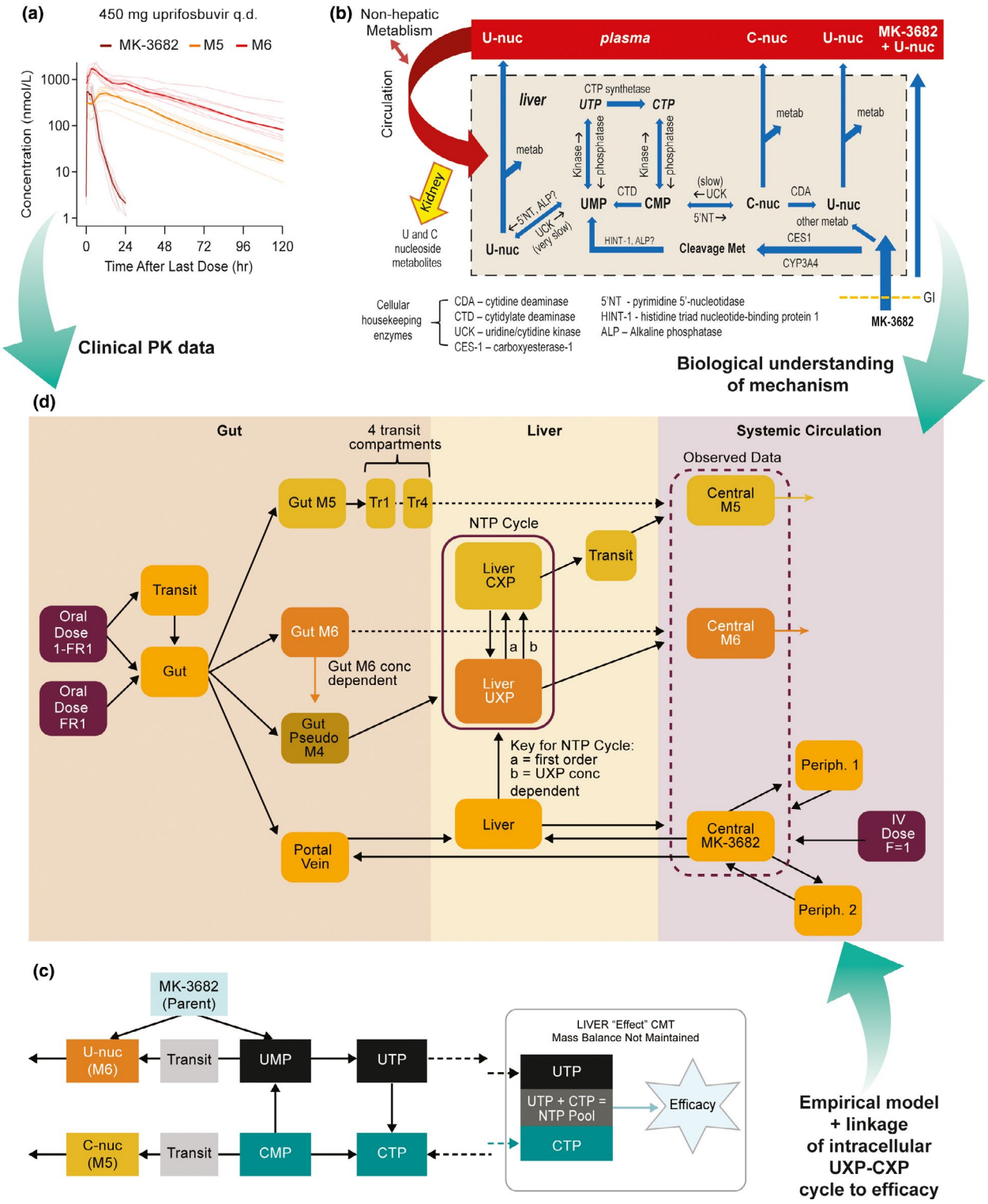

FIGURE 1 Combining clinical PK, biological understanding of uprifosbuvir metabolism, and effect site kinetics in one minimal physiologically based PK–pharmacodynamic model. (**a**) Raw data plot of individual uprifosbuvir, M5, and M6 concentration-time profiles at Day 7, including washout, after once-a-day dosing of the 450 mg uprifosbuvir tablet in patients with hepatitis C virus. (**b**) Anticipated metabolism by host (human) housekeeping enzymes. (**c**) Empirical model used in early model development with link to efficacy. (**d**) Schematic minimal physiologically based PK model for uprifosbuvir. C, cytidine; CMP, cytidine monophosphate; conc, concentration; C-nuc, M5; CTP, cytidine triphosphate; CXP, cytidine varieties; F, bioavailability; GI, gastrointestinal; IV, intravenous; metab, metabolite; MK-3682, uprifosbuvir; NTP, nucleoside triphosphate; periph, peripheral; PK, pharmacokinetics; q.d., once daily; Tr1, transit 1; Tr4, transit 4; UMP, uridine monophosphate U-nuc, M6; U, uridine; UTP, uridine triphosphate; UXP, uridine varieties

CTP, cytidine monophosphate (CMP), and back into UMP. The phosphorylation and dephosphorylation steps are bidirectional via kinase and phosphatase enzymes, respectively. CMP can be metabolized into M5 and subsequently M6, both of which can then enter the general circulation. Intrahepatic concentrations of UMP, UTP, and CTP are unmeasurable in human, and measured levels of plasma analytes (uprifosbuvir, M5, and M6) thus can be leveraged to potentially infer active intrahepatocyte concentrations that could be linked to VL reduction. However, a number of other plausible routes complicate this picture, causing the observed plasma concentrations to result from not only "active production" (conversion via the active analytes at the site of action) but also "inactive production" as well (production or excretion via routes without involving the active analytes). Examples include the following:

a. After absorption, a fraction of uprifosbuvir can enter the general circulation directly and be converted to M6 (via M4) there without contributing to intrahepatic CTP or UTP active levels.
b. Within the gastrointestinal tract, M6 could be produced from uprifosbuvir via hydrolysis in the lumen or via carboxyesterase and cytochrome P450 (CYP) 3A4–mediated metabolism when passing enterocytes. Cleavage product M4 is probably formed as an intermediate between uprifosbuvir and M6, possibly not reflecting the active compound.
c. Transport across the gastrointestinal wall (including P-glycoprotein transporters) and/or gastrointestinal metabolism are possibly saturable, which might cause changes in the relative fraction of uprifosbuvir that is converted into intrahepatic CTP and UTP.
d. M5 and M6 themselves could be metabolized and excreted within hepatocytes without appearing in the general circulation.

2. Results from critical clinical studies came in (including intravenous [i.v.] administration of uprifosbuvir, and coadministration with itraconazole in healthy volunteers and patients with HCV), with some unanticipated PK and efficacy results. PK profiles after once-a-day (q.d.) tablet doses by mouth (p.o.) showed a rapidly increasing and declining uprifosbuvir concentration over time. The M6 profiles, however, showed multiple peaks indicating a combination of quick and slow production processes (Figure 1a). This would be consistent with the hypothesis of production of M6 via both active (via CTP or UTP cycle) and inactive routes (e.g., in the gut). This hypothesis is supported by the fact that the first peak was absent when coadministering itraconazole, which would suggest a change in the relative availability of uprifosbuvir for the active versus inactive routes. While waiting for additional PK information, a preliminary kinetic–PD (K-PD) model was being developed, aiming to describe the observed data and establish the dose–response relationship. Although the K-PD model did not account for the complex metabolism hypothesis as noted previously, it was able to describe individual VL profiles adequately by linking uprifosbuvir doses to VL reduction via an effect compartment.[1] Hence, the model-derived empirical Bayesian estimates representing viral inhibition (ε, Equation 1) were considered useful as individual effect estimates that could be used to inform the intrinsic PK driver in future exposure–response evaluations.

$$\varepsilon = E_{max} \times \frac{C_{50}^{N}}{EC_{50}^{N} + C_{50}^{N}} \quad (1)$$

The combination of the formulated hypotheses, *in vitro* information, and the availability of clinical data led to the insight that a simple 1:1:1 relationship between plasma analytes (uprifosbuvir/M5/M6), NTP, and the resulting VL decline could not be assumed. Crucially, we did not know quantitatively which moiety (CTP or UTP) was responsible for which fraction of VL reduction *in vivo*. Therefore, we started a collaborative modeling exercise specifically geared toward identifying key steps in uprifosbuvir metabolism, allowing the distinction between active and inactive production routes of M5 and M6 formation. This was followed by selection of the nucleoside with the best predictive power for VL reduction and identification of intrinsic and extrinsic factors that might affect the dose–response relationship such as formulation, disease state, and drug–drug interactions (DDIs).

The modeling strategy was iteratively discussed among the members of the development team and was ultimately guided and supported by the availability of data (Figure 1a) and understanding of drug metabolism pathways (Figure 1b). Initially, model development was limited to plasma concentrations after p.o. administration in healthy volunteers and patients with HCV, including data after coadministration with itraconazole (healthy volunteers only). At this early stage, we considered a full physiologically based PK (PBPK) model unrealistic due to a scarcity of informative data. Furthermore, given the complex metabolism pathway and unmeasurable active moiety in the liver, the commercially available PBPK platforms, such as SimCYP and GastroPlus, were considered inadequate for our objectives. Thus, the starting point was an empirical model in which the kinetics of uprifosbuvir, M5, and M6 were incorporated, including compartments representing intrahepatic NTP concentrations, which should ultimately be linked to efficacy data (Figure 1c). As more data became available, the approach shifted to a PBPK model, characterized by an in-depth investigation of specific pathways including a separation of gut versus liver processes

(Figure 1d). Finally, an exposure–response model was set up to test UXP and CXP predictions from the PBPK model versus ε values from the original K-PD model in an attempt to find out whether UXP, CXP, or a combination is the best predictor of VL reduction.

Data

Table 1 contains an overview of all data used in the creation of the empirical model (Step 1), creation of the minimal PBPK model (Step 2), augmenting the minimal PBPK model with itraconazole DDI data (Step 3), and finally evaluation of the best predictor for observed VL reduction (Step 4). In Table S1, an overview of the corresponding study designs is provided.

Computation

Minimal PBPK modeling was done using the NONMEM software package (Version 7.2; Icon Development Solutions, Ellicott City, MD) with a Compaq Visual Fortran compiler (Version 6.6; Compaq Computer Corp., Houston, TX) and Perl-speaks-NONMEM (Version 4.6.0[2]). Creation of diagnostic plots and postprocessing of NONMEM output was done using R (Version 3.3.2[3]). Exploratory simulations were done using Berkeley-Madonna (Version 8.3.18; Berkeley Madonna Inc., University of California, Berkeley, CA). To obtain 95% confidence intervals for all parameters, models from Steps 2f, 3, and 4 (see Table S2) were rerun using NONMEM Version 7.5 (Icon Development Solutions).

RESULTS

Step 1: empirical PK model in healthy volunteers after p.o. dosing

Although not all data were initially available (thereby making a separation between gut and liver processes challenging), model-based support was started to get a general idea of the relevance of different hypothesized metabolic pathways. To support the model, a graphical evaluation was done of plasma uprifosbuvir, M5, and M6 concentration-time profiles in healthy volunteers after oral administration. The PK profiles showed a rapidly declining uprifosbuvir curve, whereas M5 and particularly M6 showed signs of both quick and slow production (reflecting "inactive" gut vs. "active" liver processes), resulting in two distinct peaks over time in some but not all subjects (Figure 1a). Separation of "inactive" gut versus "active" liver pathways was considered important for ultimately linking the model to viral inhibition. This was implemented as one pathway directly from uprifosbuvir to M6 (representing gut production) and one via a transit mechanism (representing hepatic production). In an attempt to include both M5 and M6, taking into account the presumed biological link between their hepatic production mechanisms, a simplified (unidirectional) UMP-UTP-CMP-CTP loop was added (Figure 1c).

This model was successful in the sense that two M6 peaks could be described while describing the delayed formation of M5 resulting in a peak around 16 h postdose. Unfortunately, it was unstable, resulting in poor minimization and poor precision of parameter estimates. The instability could not be overcome by simplifying the model by fixing initial parameters, equalizing volumes of distribution, and so on. We concluded that gut and liver processes could not be differentiated, which is to be expected when dealing with data after p.o. administration in the absence of i.v. data. Another drawback of the empirical model is the absence of identifiable UTP versus CTP concentrations: the simplified implementation of the UMP-UTP-CMP-CTP loop precludes separation of these compounds, which was considered crucial to answer questions about the most appropriate exposure–response relationship. Based on these considerations, the decision was made between all stakeholders to put further modeling on hold, awaiting the opportunity to construct a more physiology-based model (i.e., separating gut and liver metabolism, identifying bioavailability fractions and relative fractions, and specifically identifying the MP-UTP-CMP-CTP loop) when data from studies with i.v. administration became available.

Step 2: physiology-based PK model in healthy volunteers and patients with HCV, p.o., and i.v. dosing

Step 2 of the model-based support involved a stepwise and data-driven expansion of a physiology-based model in which newly available data were integrated as they became available.

This process was founded in careful graphical evaluation of uprifosbuvir, M5, and M6 plasma concentration profiles and model predictions in combination with hypothesis-based testing of potential changes to the metabolic pathways that are represented in the model. From the modeling perspective, this required intensive trial and error in NONMEM and Berkeley-Madonna to assess the impact of different potential model improvements on overall goodness of fit. Model development involved intensive feedback between modelers, clinicians, and preclinical members of the development team pertaining to comparative assessment of goodness of fit, formulation of hypotheses on potential changes to the model, comparison of physiological or pharmacological plausibility and suitability of different hypotheses, and the ultimate

TABLE 1 Overview of data sets used in the analysis

Step	Data	Analytes	Subjects	Clinical studies
Step 1: empirical model	150–600 mg SD tablet ($N = 53$), 300–750 mg MD tablet ($N = 35$)	Uprifosbuvir + M5 + M6	HV	P002, P003, P010, P013, P026
Step 2: physiology-based PK model				
(a) Uprifosbuvir i.v.	25 mg i.v. ($N = 14$)	Uprifosbuvir	HV	P026
(b) Uprifosbuvir i.v. + p.o. (tablet)	Data from Step 2a + 450 mg SD tablet ($N = 12$)	Uprifosbuvir	HV	P026
(c) Combined (uprifosbuvir, M5, & M6) i.v.[a]	25 mg i.v. ($N = 14$)	Uprifosbuvir + M5 + M6	HV	P026
(d) Combined i.v. + p.o. SD p.o. (tablet), BA study only	Data from Step 2c + 450 mg SD tablet ($N = 12$)	Uprifosbuvir + M5 + M6	HV	P026
(e) Combined i.v. + p.o. SD p.o. (tablet)	Data from Step 2c + 150–900 mg SD tablet ($N = 59$)	Uprifosbuvir + M5 + M6	HV	P003, P010, P013, P026
(f) Combined i.v. + p.o. SD & MD p.o. (tablet)[b]	Data from Step 2c + 150–900 mg SD tablet ($N = 59$) + 300–750 mg MD tablet ($N = 35$)	Uprifosbuvir + M5 + M6	HV	P002, P003, P010, P013, P026
(g) Combined i.v. + p.o. SD & MD p.o. (tablet & capsule)	Data from Step 2f + 50–300 mg SD and 300 mg MD capsule ($N = 47$, HV) + 300–450 mg MD tablet ($N = 16$, HCV) + 50–300 mg SD and 50–400 mg MD capsule ($N = 64$, HCV)	Uprifosbuvir + M5 + M6	HV + patients with HCV	P001, P002, P003, P010, P013, P026
Step 3: itraconazole DDI	Data from Step 2g + 300 mg SD tablet together with 200 mg MD itraconazole ($N = 11$, HV) + 300 mg MD tablet together with 200 mg MD itraconazole ($N = 8$, HCV)	Uprifosbuvir + M5 + M6	HV + patients with HCV	P001, P002, P003, P010, P013, P026
Step 4: Link exposure to VL	All patients with HCV ($N = 88$): 300–450 mg MD tablet ($N = 16$) +50–300 mg SD and 50–400 mg MD capsule ($N = 64$) + 300 mg MD tablet together with 200 mg MD itraconazole ($N = 8$)	ε values from K-PD model	Patients with HCV	P001

BA, bioavailability; DDI, drug–drug interaction; HCV, hepatitis C virus; HV, healthy volunteers; i.v., intravenous; K- PD, kinetic–pharmacodynamic; MD, multiple dose; PK, pharmacokinetics; p.o., by mouth; SD, single dose; VL, viral load.

[a]Uprifosbuvir i.v. parameter estimates from this step were fixed for subsequent model development steps.

[b]Parameter estimates from this step were fixed for subsequent model development steps.

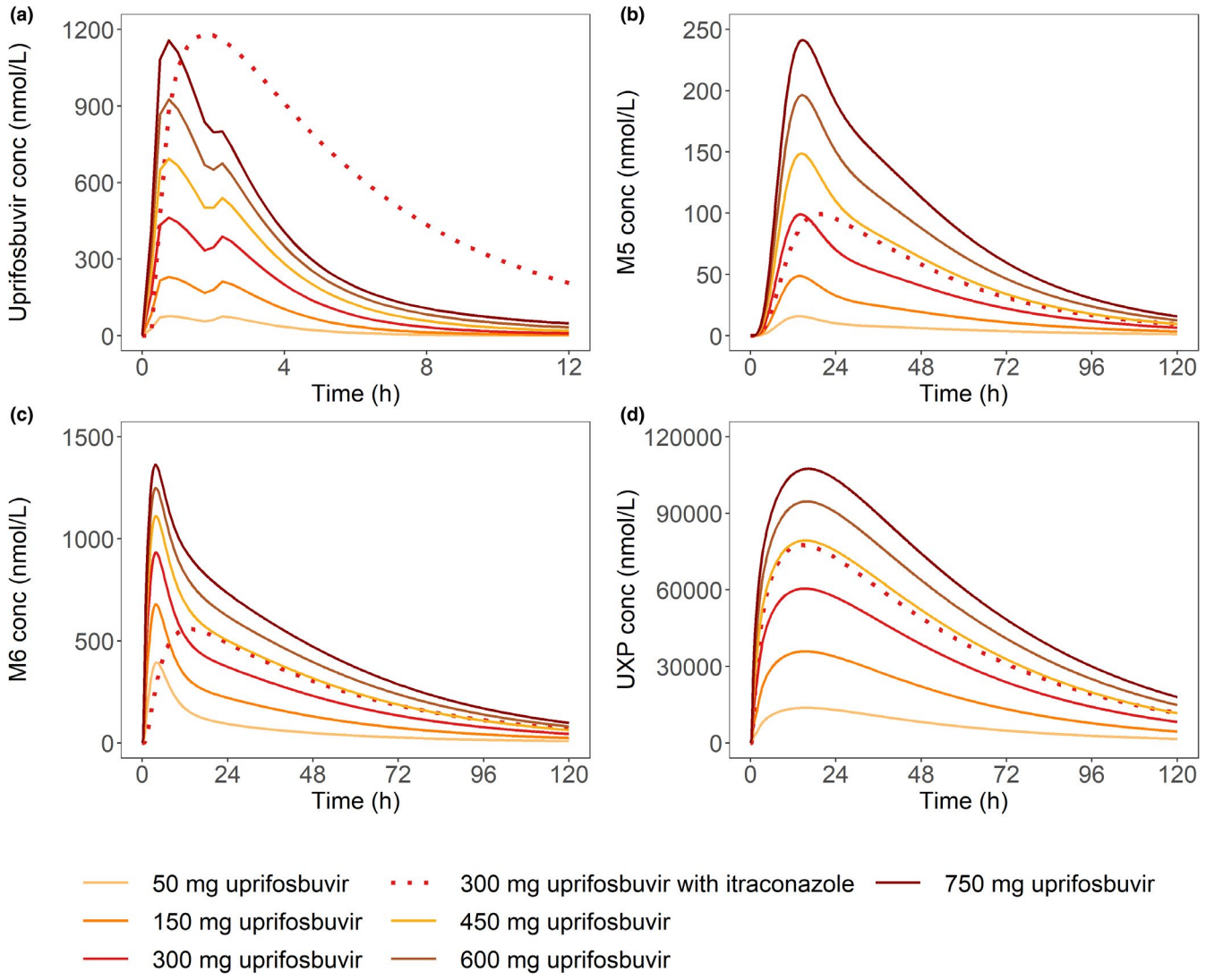

FIGURE 2 Minimal physiologically based model-predicted pharmacokinetic profiles for different single uprifosbuvir tablet dose levels for (**a**) uprifosbuvir, (**b**) M5, (**c**) M6, and (**d**) UXP. The impact of itraconazole coadministration is shown at 300 mg. UXP, uridine phosphates

decision on which (pre-)clinical information and pathways to include.

Our starting point was a PBPK model published by Brill et al. describing the PK of midazolam and its main metabolite in obese subjects with and without bariatric surgery.[4] Although it refers to an entirely different indication and drug class, there are many similarities with uprifosbuvir PK: (a) the model was based on i.v. and p.o. dosing of the parent compound; (b) production of the metabolite occurs primarily in the liver, but also happens in the gut wall via CYP3A enzymes; (c) the model was built on observed parent and metabolite concentrations in plasma, but both are affected by gut and liver processes (cf. "active" and "inactive" production of uprifosbuvir metabolites); and (d) the model was built via hypothesis testing—different blood flow scenarios were tested and evaluated to find the optimal model configuration with respect to goodness of fit and physiological plausibility.

The data used to create the PBPK model are described per modeling step in Table 1. An overview of modeling steps and hypotheses can be found in Table S2. The resulting PBPK model is provided in Figure 1d. Relevant physiological parameters (blood flows, vein and liver volume, etc.) were taken from literature[5–7] and/or obtained from experiments (blood:plasma ratio, fractions unbound, and gut-wall permeability). In short, the inclusion of data after i.v. administration allowed a description of uprifosbuvir, M5, and M6 PK in the absence of gut metabolism under the assumption that there is no enterohepatic recirculation. This facilitated the description of not just processes in the liver and general circulation, but also the uprifosbuvir bioavailability and absorption profiles, which were ultimately described via a combined fast and slow absorption process (Step 2a and 2b; Figure 1a). By assuming that uprifosbuvir dose is the only variable that determines total NTP in the body, we could use i.v. and p.o. data to calculate the relative contribution of the hepatic versus the gut route of NTP production.

To get a clear picture of the hepatic processes involved in uprifosbuvir metabolism, M5 and M6 data after i.v. administration were added and modeled in the absence of uprifosbuvir p.o. data (Step 2c). Although inclusion of i.v. M5 and M6 data helped fill in knowledge gaps, description of the full UMP-UTP-CTP-CMP cycle was not supported by the available data, prompting a collapse to UXP and CXP compartments. Addition of uprifosbuvir, M5, and M6 data after single-dose (tablet) p.o. administration allowed the identification of M5 and M6 production in the gut and prompted fine-tuning of the model (Steps 2d and 2e). A concentration-dependent elimination of M6 from gut captured the dose dependence of the first M6 peak (Figure 2c) without negatively affecting goodness of fit for uprifosbuvir and M5. The inclusion of pseudo-M4 in the gut was ultimately the only viable way to account for additional delayed (10–24 h) M5 and M6 production.

The model established on single-dose p.o. data was extended with multiple-dose p.o. data, which provided information on nonlinearities in the conversion from CXP to UXP and subsequent M6 formation (Step 2f). The elimination rate did not seem to change between single-dose and multiple-dose scenarios, but accumulation was lower than expected based on clearance alone, which was successfully included in the model.

Finally, applicability of the model to data of patients with HCV was investigated. This also involved quantification of formulation differences. Graphical exploration of plasma uprifosbuvir, M5, and M6 concentrations after p.o. administration (capsule formulation) in patients with HCV (Step 2g) revealed that the uprifosbuvir absorption profile and bioavailability were slightly different between tablets and capsules. Second, there was a bias in random effect estimates of M6 gut elimination, which could be corrected by reestimating parameters in the concentration-dependent M6 gut elimination rate. Last, plasma M5 was underpredicted in patients with HCV, which was hypothesized to be the result of a difference in hepatic elimination between healthy volunteers and patients with HCV and would be consistent with a higher incidence of impaired liver function in patients with HCV.[8]

The resulting model was considered adequate because the model provided separation of hypothesized CXP and UXP concentrations and allowed estimation of key model parameters describing "active" and "inactive" M5 and M6 production routes. The prediction of typical PK and variability of uprifosbuvir, M5, and M6 plasma concentrations after SD and MD p.o. in healthy volunteers and patients with HCV (Figure 3) was considered acceptable for the purpose of the analysis.

Step 3: inclusion of itraconazole DDI data

Data from an itraconazole DDI study in healthy volunteers was available from the start, but initially not included in the minimal PBPK model. Based on the plasma concentration-time data, coadministration with itraconazole resulted in a delayed time to reach maximum uprifosbuvir plasma concentration and a large increase in uprifosbuvir exposure in the absence of increased plasma M5 and M6 concentrations. In fact, initial M5 concentrations were lower, and the first M6 peak was almost absent during itraconazole coadministration (Figure 2). This pattern would match a situation in which gut conversion of uprifosbuvir was reduced by CYP3A4 or P-gp inhibition,[9] resulting in higher availability of uprifosbuvir for hepatic conversion. With higher uprifosbuvir bioavailability, CXP and UXP production and ultimately viral inhibition would be increased. An additional itraconazole DDI study in patients with HCV was done to investigate this. The results confirmed that in the presence of itraconazole the onset of viral inhibition was faster and the effect lasted longer compared to uprifosbuvir administered alone (Figure 3).

Inclusion of the itraconazole DDI data in the established minimal PBPK model could be done by including plausible covariate effects: in the presence of itraconazole uprifosbuvir absorption was slower, gut and intrinsic clearances were reduced and the gut M6 route was essentially blocked, allowing a (previously impossible) differentiation between gut and liver pathways of M6 production. Based on the visual predictive checks for uprifosbuvir, M5, and M6 plasma concentrations in healthy volunteers and patients with HCV in the presence of itraconazole (Figure 4), the typical PK and variability was adequately captured for the purpose of the analysis. The model from this step is considered the final minimal PBPK model and was used to explore the exposure response. Detailed information on the model equations, model parameters, and covariate effects are provided in the supplementary information.

Step 4: linking predicted UXP and CXP concentrations to viral inhibition

The final step of the analysis was the exploration of the exposure–response relationship by comparing predicted CXP and/or UXP to the individual viral inhibition (ε) estimates as a measure of VL reduction. In a way this can be considered an external validation of the minimal PBPK model, as VL data nor model parameters of the K-PD model were part of the minimal PBPK model development. The post hoc estimates from the final PBPK model were used to extract individual NTP (UXP and CXP) concentrations, which were linked to the viral inhibition parameter ε values that describe the drop in VL via an E_{max} function (see Equation 1). In general, higher uprifosbuvir doses (and itraconazole coadministration) lead to a stronger and more sustained reduction in VL, which corresponded with higher predictions of UXP and CXP concentrations. The best predictor of viral

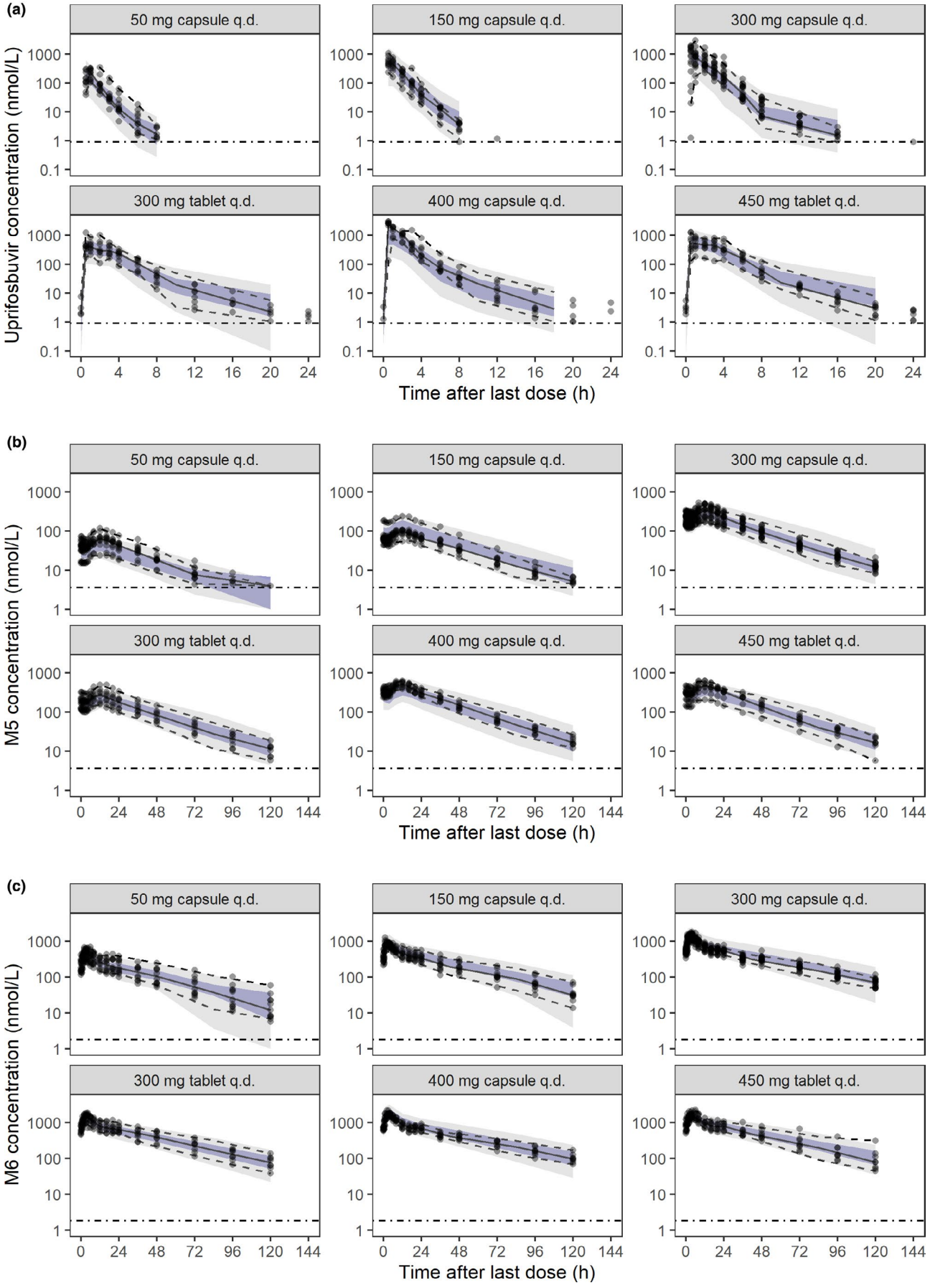
(a)
50 mg capsule q.d.
150 mg capsule q.d.
300 mg capsule q.d.
300 mg tablet q.d.
400 mg capsule q.d.
450 mg tablet q.d.
Uprifosbuvir concentration (nmol/L)
1000
100
10
1
0.1
0 4 8 12 16 20 24
Time after last dose (h)
(b)
50 mg capsule q.d.
150 mg capsule q.d.
300 mg capsule q.d.
300 mg tablet q.d.
400 mg capsule q.d.
450 mg tablet q.d.
M5 concentration (nmol/L)
1000
100
10
1
0 24 48 72 96 120 144
Time after last dose (h)
(c)
50 mg capsule q.d.
150 mg capsule q.d.
300 mg capsule q.d.
300 mg tablet q.d.
400 mg capsule q.d.
450 mg tablet q.d.
M6 concentration (nmol/L)
1000
100
10
1
0 24 48 72 96 120 144
Time after last dose (h)

FIGURE 3 Visual predictive check (VPC)s for uprifosbuvir, M5, and M6 after multiple dosing of uprifosbuvir by mouth in patients with hepatitis C virus. VPCs for (**a**) uprifosbuvir, (**b**) M5, and (**c**) M6 after multiple dosing of uprifosbuvir by mouth in patients with hepatitis C virus. Plots are stratified by dose and formulation. Black line, median observed data; black dashed lines, 5th and 95th percentiles of the observed data; dark blue area, 95% prediction interval of the simulated median; light gray area, 5th and 95th percentiles of the 90% prediction interval; black dashed line, lower limit of quantification. q.d., once a day

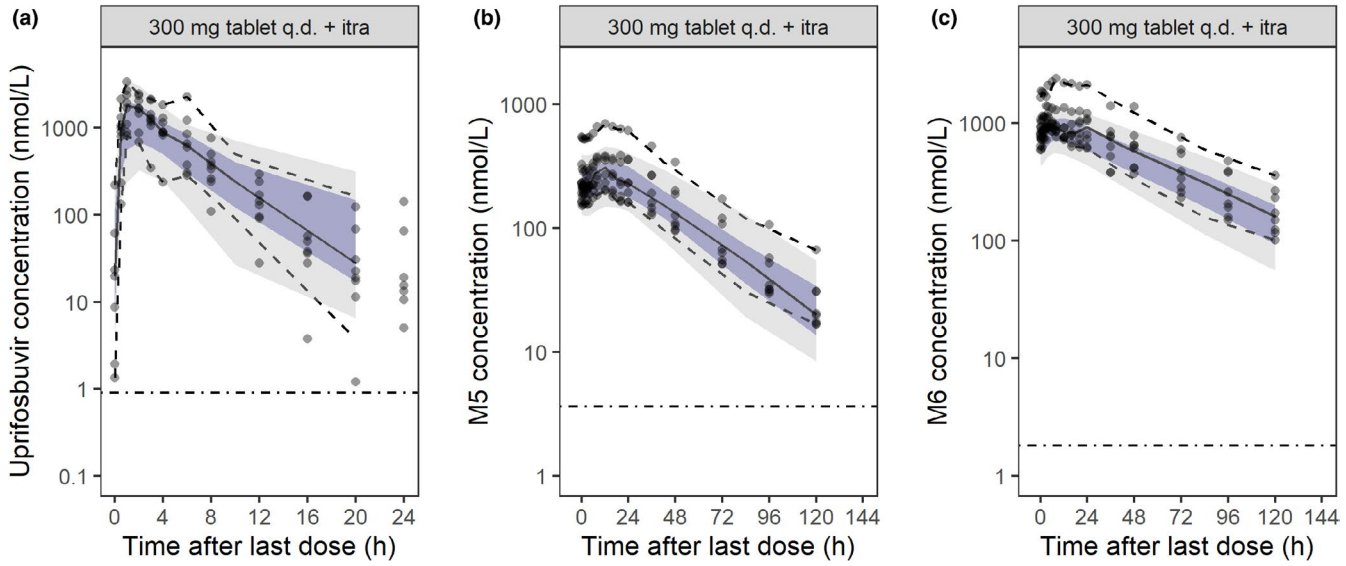

FIGURE 4 Visual predictive check (VPC)s for uprifosbuvir, M5, and M6 after multiple dosing of uprifosbuvir by mouth in the presence of itraconazole in patients with hepatitis C virus. VPCs for (**a**) uprifosbuvir, (**b**) M5, and (**c**) M6 after multiple dosing of uprifosbuvir by mouth in the presence of itraconazole in patients with hepatitis C virus. Black line, median observed data; black dashed lines, 5th and 95th percentiles of the observed data; dark blue area, 95% prediction interval of the simulated median; light gray area, 5th and 95th percentiles of the 90% prediction interval; black dashed line, lower limit of quantification. itra, itraconazole; q.d., once a day

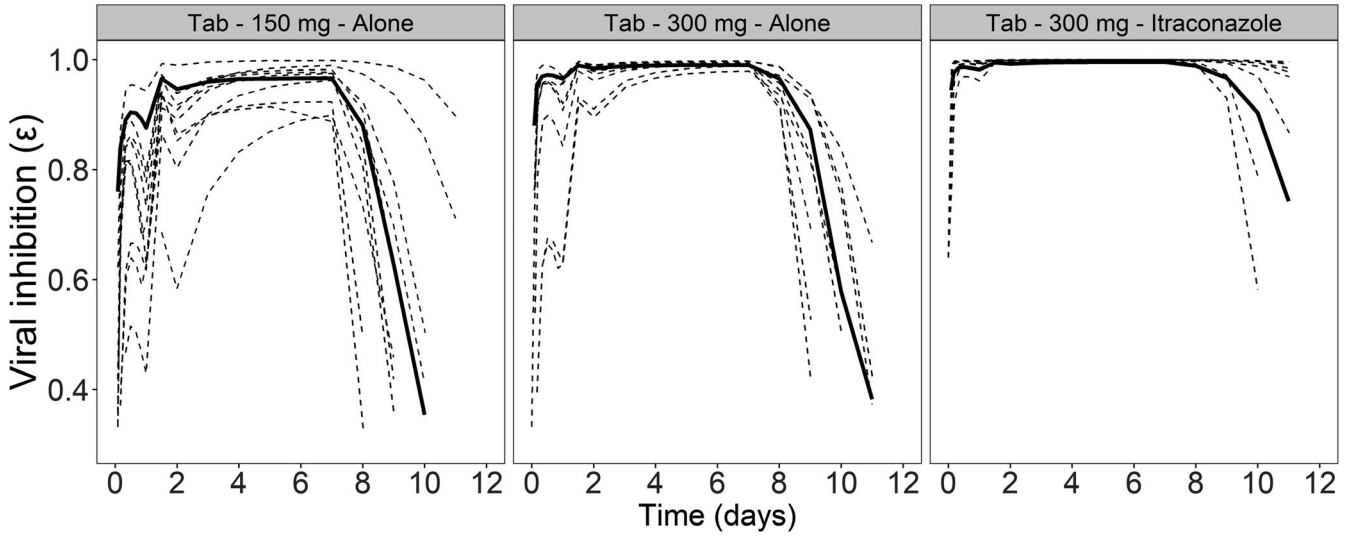

FIGURE 5 Minimal physiologically based pharmacokinetic–pharmacodynamic (PBPK-PD) model fits of viral inhibition (ε) versus time data. Minimal PBPK model-predicted uridine equivalent concentrations were linked to the ε over time data taken from a kinetic–pharmacodynamic (K-PD) model previously developed to link dose to viral inhibition in dynamic manner. Solid lines, typical minimal PBPK-PD model predictions; dashed lines, K-PD model-predicted ε versus time profiles. UXP, uridine phosphates

inhibition was UXP, which was included in the final PK/PD model (over CXP, the sum of UXP and CXP, and the sum of UXP and an estimated fraction of CXP to account for potential differences in UXP and CXP potency). Despite some overprediction of the onset of the effect in the 50-mg and 150-mg dose groups, the model seemed to capture the UXP versus ε relationship (Figure 5). Although the quality of the description of VL reduction was sufficient for the goals of this analysis, exploration of potential causes for underprediction and overprediction was considered desirable. There were some signs of proteresis or hysteresis in a subset of individual exposure–response curves, but the available data could not support inclusion of a time-delayed effect using the current model structure. Potential modifications (including a direct link between VL and UXP or CXP predictions) and informative study designs were hypothesized, but rendered immaterial by the decision to terminate development of this compound. The model from this step is considered the final minimal PBPK-PD model. The parameter estimates and the NONMEM control stream are provided in the supplementary information.

General description of the base minimal-PBPK model

The model roughly consists of gut, liver, and systemic circulation blocks (see Figure 1d).

Gut

In gut, uprifosbuvir is split into two fractions, of which one fraction (FR1) is rapidly absorbed after a short lag time and the remaining fraction (1-FR1) is absorbed either with a relatively fast absorption rate (decreased rate with increasing dose) and a lag time of approximately 2 h or via a relatively slow process via a transit compartment.

Based on the model about 14% of uprifosbuvir dose is estimated to reach the liver unchanged. The unabsorbed fraction of uprifosbuvir dose (86%) was assumed to be metabolized into M5 (11%), M6 (52%), and pseudo-M4 (37%), which represents uprifosbuvir that is metabolized in the gut and taken up as M4 before reaching the hepatic UXP-CXP cycle. A relatively small fraction of uprifosbuvir metabolized in gut is absorbed via the gut M5 route in the model. As gut formation of M5 appeared to be relatively slow, it was described via a series of four transit compartments. Unlike the PK of uprifosbuvir and M5, which appeared to be dose proportional, PK for M6 was not dose proportional. The observed nonlinearity in gut M6 absorption was described by a gut M6 compartment from which M6 was either absorbed with first-order absorption rate or eliminated with a gut M6 concentration-dependent elimination rate. This could describe the relative decrease in height of the M6 peak at higher dose levels.

Liver and systemic circulation

Uprifosbuvir disposition was described using a central compartment and two peripheral compartments of equal volume. All uprifosbuvir metabolized in liver was assumed to be converted to either M5 or M6 via a simplified NTP route. Basically, the UMP-UTP-CTP-CMP cycle was reduced to two compartments: UXP (UMP + UTP) and CXP (CMP + CTP). For M5, a transit compartment was included to describe the delay in M5 formation. All distribution and metabolic processes related to M5 and M6 were modeled as first-order processes. To describe the accumulation of M5 and M6 toward steady state for the oral data, a concentration-dependent rate from UXP to CXP was included in the model. The higher the concentrations in the UXP compartment, the faster the concentration-dependent rate from UXP to CXP.

Finalization of the project

At this stage in the analysis, development of this compound was discontinued for strategic reasons. Nevertheless, the developed PBPK model with the link to VL reduction has provided valuable understanding of the complex hypothesized metabolism of uprifosbuvir and of the relationship between plasma PK and liver NTP. In addition, it allowed an evaluation of the impact of treatment of patients with HCV versus healthy volunteers, the capsule versus tablet formulation, and of concomitant itrazonazole administration.

This project provided a learning opportunity beyond clarification of the main metabolic pathways of uprifosbuvir. Originally, it was focused on fitting a minimal PBPK model that helps answer a few concrete questions on the impact of intrinsic and extrinsic factors on uprifosbuvir PK and the expected drop in VL. During the project, the goals evolved: the poor identifiability of crucial pathways prompted multidisciplinary discussions on the plausibility of different hypothetic metabolic routes. In turn, evaluation of the accuracy of model-based predictions (a form of hypothesis testing) informed the development team on the physiological fate of uprifosbuvir and its main metabolites. As a result, this project turned into a collaborative learning exercise, focused toward gaining a deeper understanding of the data from multiple perspectives from a variety of functional backgrounds. Insights gained from this process can probably be reused in forming optimal collaborations (and PK/PD models) for a variety of compounds under investigation, not limited to uprifosbuvir or similar antiviral compounds. This approach is broadly replicable, especially in

cases that share some commonality with the case described here, including dosing of prodrugs, alternative formulations, situations where PK at the site of action is not directly measurable, and cases where biomarker or efficacy data can be generated in clinical pharmacology studies. Beyond the direct scientific application, the thinking process and close collaboration between multiple disciplines could serve as an educational example in the general MIDD paradigm.

DISCUSSION

The successful completion of this analysis would not have been possible without intensive cooperation between different disciplines (Figure 6) and the incorporation of new information over time. This process became possible by the mutual willingness to reevaluate goals during modeling and by reevaluation of preconceived hypotheses on metabolism or mechanism of action. The complexity of this project prompted a multitude of reflection moments during analysis in which discussions (internal within the modeling team and external with representatives of different disciplines) were necessary to improve understanding of the system. A number of lessons might be useful for future projects:

a. Useful information was obtained with brainstorm sessions and joint investigation of observed parent and metabolite profiles as well as the results of exploration of different hypotheses. Joint discussion of results often leads to a comprehensive list of options that can be classified based on physiological plausibility, expected success (taking into account model and data limitations), and preclinical evidence. This could focus model development and can prevent investing in dead ends (from a biochemical perspective), futile modeling attempts, or additional studies with limited additive value.
b. This type of collaboration requires deep engagement from all participants and frequent dialogue. Planning of fixed periodical meetings is useful with ad hoc shorter meetings as well as an elaborate kick-off meeting in which all participants are informed on the content of available data, limits of available models, and the level of knowledge and evidence on individual metabolic pathways.
c. Modeling is often seen as the conclusion of a serial process in which available information is used until no more information can be extracted from the data. At some point during the uprifosbuvir analysis, however, model development was halted awaiting new data, which is an unusual step. The uprifosbuvir case illustrates that modeling can be more effective when seen as an iterative process alongside experimentation. From this perspective, a gap in the model is not seen as a problem that needs to be worked around (by tweaking parameterization, inputting literature parameters, accepting descriptive items where physiological solutions might be viable, etc.), but an opportunity to engage the development team and jointly find a way to get the required information.
d. Multiple data sources were required to fill in the blanks: clinical data after i.v. administration of uprifosbuvir in

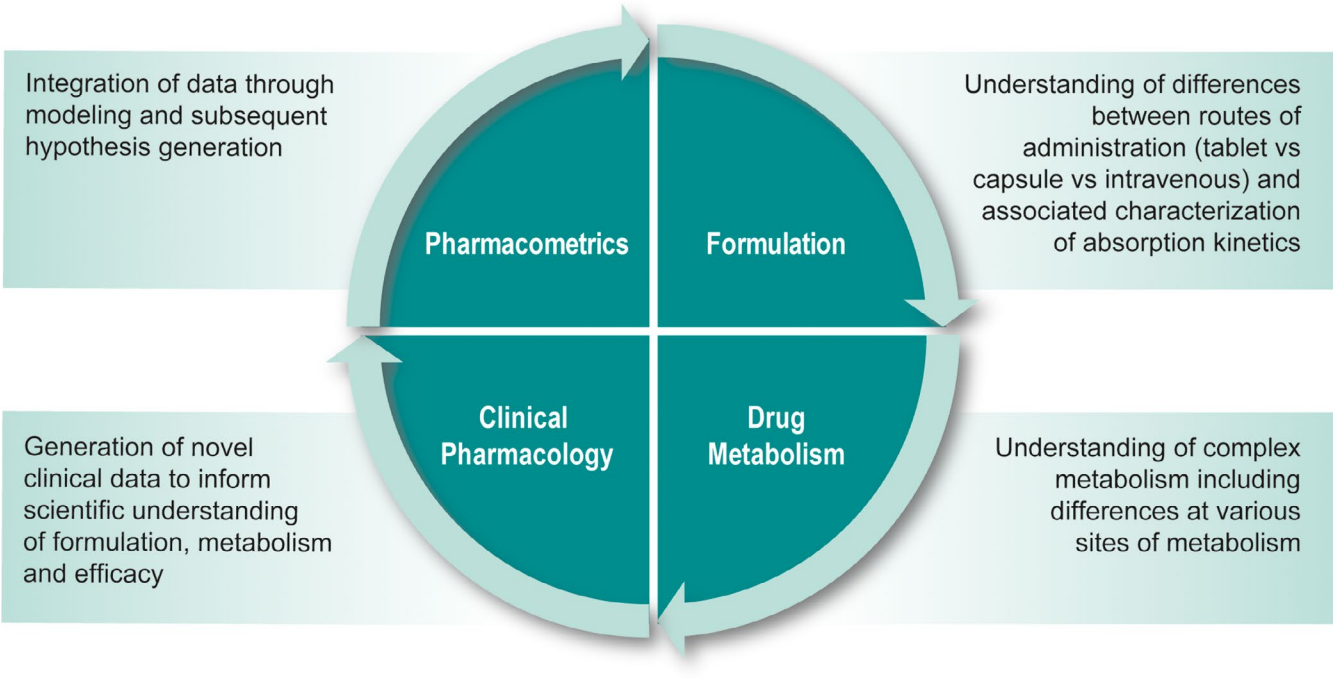

FIGURE 6 Interplay between modeling, formulation, drug metabolism, and clinical pharmacology during model development

particular were critical to separate gut versus liver processes and prompted a shift toward a PBPK approach. Although complicated, i.v. administration of metabolites M5 and M6 would have been useful in supporting or dismissing certain metabolic routes. In cases where there is a likely link between metabolites and effect site concentrations, additional studies with these metabolites at an early stage could be worthwhile additions to the spectrum of available data.

e. The value of the DDI data went beyond a simple covariate analysis to support potential dose adjustments in clinical practice; they provided valuable input on the contribution of different metabolic pathways. This provides a strong incentive to include DDI data as an integral part of the model-building process instead of an afterthought on a more or less completed model to evaluate the relevance of potential covariate effects. The fact that the increased efficacy in patients with HCV during itraconazole treatment could be captured by the model showed that the hypothesized metabolism pathway was directionally correct and the proposed PK model was able to provide the insight regarding the quantitative differentiation of the productive and unproductive routes of metabolite formation. This provides confidence in the model and the metabolic routes therein, but also in the overall approach.

ACKNOWLEDGMENTS

The authors acknowledge Pratik Bhagunde (employed at Merck Sharp & Dohme Corp., a subsidiary of Merck & Co., Inc., Kenilworth, NJ, USA, at the time of this project) for development of the kinetic–pharmacodynamic model and Peter Vis (LAP&P) for his contributions to the discussions throughout the project.

CONFLICT OF INTEREST

L.A., W.G., F.K., R.M., and M.L.R. are employees of Merck Sharp & Dohme Corp., a subsidiary of Merck & Co., Inc., Kenilworth, NJ, USA. P.B., M.J.A., and T.M.P. are employees of LAP&P Consultants BV and performed this work for Merck & Co Inc. as part of a consultancy contract.

REFERENCES

1. Bhagunde P, Rizk ML, Marshall W, Butterton J, Gao W. Viral dynamics modeling of MK-3682 monotherapy in HCV-infected patients. *J Pharmacokinet Pharmacodyn*. 2015;42:S104-S105.
2. Lindbom L, Pihlgren P, Jonsson EN. PsN-Toolkit–a collection of computer intensive statistical methods for non-linear mixed effect modeling using NONMEM. *Comput Methods Programs Biomed*. 2005;79(3):241-257. https://doi.org/10.1016/j.cmpb.2005.04.005.
3. R Development Core Team. *R: A language and environment for statistical computing*. Vienna, Austria: R Foundation for Statistical Computing. http://www.R-project.org. Published 2008. Accessed March 17, 2021.
4. Brill MJ, Välitalo PA, Darwich AS, et al. Semiphysiologically based pharmacokinetic model for midazolam and CYP3A mediated metabolite 1-OH-midazolam in morbidly obese and weight loss surgery patients. *CPT: Pharmacometrics Syst Pharmacol*. 2016;5(1):20-30.
5. Yang J, Jamei M, Yeo KR, Tucker GT, Rostami-Hodjegan A. Prediction of intestinal first-pass drug metabolism. *Curr Drug Metab*. 2007;8(7):676-684. https://doi.org/10.2174/138920007782109733
6. Davies B, Morris T. Physiological parameters in laboratory animals and humans. *Pharm Res*. 1993;10(7):1093-1095. https://doi.org/10.1023/a:1018943613122
7. Williams LR, Leggett RW. Reference values for resting blood flow to organs of man. *Clin Phys Physiol Meas*. 1989;10(3):187-217. https://doi.org/10.1088/0143-0815/10/3/001
8. Smolders EJ, de Kanter CT, van Hoek B, Arends JE, Drenth JP, Burger DM. Pharmacokinetics, efficacy, and safety of hepatitis C virus drugs in patients with liver and/or renal impairment. *Drug Saf*. 2016;39(7):589-611. https://doi.org/10.1007/s40264-016-0420-2
9. Talavera Pons S, Boyer A, Lamblin G, et al. Managing drug-drug interactions with new direct-acting antiviral agents in chronic hepatitis C. *British J Clin Pharmacol*. 2017;83(2):269-293. https://doi.org/10.1111/bcp.13095.

SUPPORTING INFORMATION

Additional supporting information may be found online in the Supporting Information section.

How to cite this article: van den Berg P, Gao W, Ahsman MJ, et al. Understanding effect site pharmacology of uprifosbuvir, a hepatitis C virus nucleoside inhibitor: Case study of a multidisciplinary modeling approach in drug development. *CPT Pharmacometrics Syst Pharmacol*. 2021;10:658–670. https://doi.org/10.1002/psp4.12644